Volume 23, No 4 | International Journal of Radiation Research, October 2025

Study of radiation attenuation properties by incorporating a zinc oxide and conjugated hole transport material into polystyrene

M. Marashdeh* and M.J. Aljaafreh

Department of Physics, College of Sciences, Imam Mohammad Ibn Saud Islamic University (IMSIU), Riyadh, Saudi Arabia

► ***Original article***

Corresponding author:
Mohammad Marashdeh, Ph.D.
E-mail:
mwmarashdeh@imamu.edu.sa

Received: May 2024
Final revised: March 2025
Accepted: May 2025

Int. J. Radiat. Res., October 2025; 23(4): 995-1001

DOI: 10.61186/ijrr.23.4.23

Keywords: *Polystyrenes, zinc oxide, half -value layer (HVL), mean free path (MFP), radiation attenuation.*

ABSTRACT

Background: This study aims to understand the impact of material composition on radiation attenuation by integrating polystyrene (PS) composites with a conjugated hole transport material (MADN) and zinc oxide (ZnO). The high atomic number of zinc is expected to enhance photon interactions, making ZnO a promising additive for radiation shielding applications. ***Materials and Methods:*** PS composites with varying concentrations of MADN (1.3%–4.5%, denoted as PM0–PM5) and ZnO (PMZnO1–PMZnO5) were prepared. Linear and mass attenuation coefficients were measured at photon energies of 59.5 keV, 661.7 keV, 1173.2 keV, and 1332.5 keV. Furthermore, the half value layer (HVL) and mean free path (MFP) were evaluated to assess the attenuation behavior at these energy levels. ***Results:*** The PM0–PM5 samples exhibited similar mass attenuation coefficients, which is attributed to the predominant presence of carbon and hydrogen atoms. The addition of ZnO significantly increased the mass attenuation coefficient, especially at lower photon energies, owing to the higher atomic number of zinc, which enhances photoelectric absorption and photon interactions. ZnO addition also reduced the HVL, particularly at 59.5 keV, where composites with higher ZnO concentrations exhibited significantly lower HVL values, indicating stronger attenuation. ***Conclusion:*** The findings highlight the crucial roles of atomic number and material density in radiation attenuation, with ZnO effectively enhancing photon attenuation in PS composites. This effect is particularly significant at lower photon energies, validating ZnO's potential as a useful additive for improved radiation shielding in PS composites.

INTRODUCTION

Nuclear and radiation technology find application in various industries, including medical diagnosis, radiation treatment, and imaging technology [1-3]. Although nuclear technology has ushered in several advancements, the resulting production of harmful nuclear radiation is a significant challenge for society. Radiation typically includes particles like photons, neutrons, and electrons, which can severely affect human health. Specifically, gamma rays and X-rays, which are characterized by high frequency and energy, possess substantial penetration capabilities that result in material ionization. Prolonged or unintended exposure to such radiation can gravely affect human health, leading to health disorders and physical deformities [4]. Therefore, the harmful effects of radiation used in daily applications must be avoided. Lead is a commonly used shielding material to protect against radiation [5] and is widely employed in building shields. However, owing to the high cost of lead and its limitations in some shielding applications, there is a need to develop new materials that are less expensive and easily available as alternatives to metals [6-12]. Shielding against neutrons and neutron-secondary products is critical and requires the use of shielding materials with a large absorption cross section. Accordingly, Low-Z elements or materials such as polymers, which are considered hydrogen-containing compounds, are the most active moderators.

Polystyrene (PS) has received considerable attention in radiation shielding research owing to its inherent flexibility, durability, and favorable mechanical properties, which make it suitable for applications requiring lightweight and adaptable shielding solutions [13-15]. Although, PS provides limited radiation protection on its own [16], it serves as a versatile base material for combination with high atomic number additives. For example, PS composites with various additives, such as lead oxide [17-19], have been developed to improve gamma and neutron radiation shielding. However, these solutions often rely on heavy metals, which pose health and environmental risks. Consequently, there is a growing interest in exploring novel additive combinations that might enhance the radiation attenuation properties of PS without the need for traditional heavy-metal-

[DOI: 10.61186/ijrr.23.4.23]

based materials.

This study introduces a new approach to radiation shielding by incorporating conjugated hole transport materials (CHTMs) into a PS matrix. CHTMs - typically used in optoelectronic devices like organic LEDs and photovoltaic cells - are recognized for their efficient hole conduction and heightened sensitivity to electric fields, properties that are traditionally valued in electronics but remain unexplored in radiation shielding applications [20-23]. When blended with PS, CHTMs can modify the polymer's physical characteristics, enhancing its electrical conductivity, thermal stability, and optical properties [24-26]. Notably, the potential of CHTMs to influence radiation attenuation behavior, particularly with gamma rays, has not yet been investigated. Thus, this research represents a pioneering effort in examining the behavior of CHTMs in radiation shielding based on the hypothesis that the unique charge-transport and stability-enhancing properties of CHTMs might offer advantages for PS composites.

Building on this innovative foundation, zinc oxide (ZnO) nanoparticles are introduced into the CHTM–PS composite and the potential synergies between these two additives are studied [27, 28]. ZnO has a high atomic number, which enhances photon interactions and increases photoelectric absorption, particularly at lower photon energies. By combining CHTMs with ZnO in varying concentrations within a PS matrix, we investigate whether the physical property enhancements of CHTMs can work synergistically with the radiation attenuation capabilities of ZnO, thereby obtaining a composite that may outperform traditional PS-based shielding materials. This novel dual-additive approach introduces a unique combination, with the aim of expanding our understanding of how PS can be tailored for effective and adaptable radiation shielding.

The effectiveness of the proposed composites is evaluated by measuring their linear and mass attenuation coefficients at photon energies of 59.5–1332.5 keV and calculating the half value layer (HVL) and mean free path (MFP). These metrics provide a comprehensive understanding of the material's radiation attenuation behavior, allowing for comparisons with the corresponding theoretical values for pure PS, which are calculated using the XCOM program. Accordingly, various insights on the impact of different CHTM and ZnO concentrations on the radiation shielding performance of PS are obtained.

Overall, this work represents a novel approach, employing PS composites for radiation protection by integrating CHTMs, hypothesizing that their charge transport and stability benefits may enhance radiation shielding. Furthermore, by combining CHTMs with ZnO, which is recognized for its photon attenuation properties, this study aims to evaluate the potential of CHTM–ZnO–PS composites for application as high-performance, lightweight radiation shielding materials. This innovative combination is expected to position these composites as a promising solution in the advancing field of radiation protection.

MATERIALS AND METHODS

Samples preparation

A pure PS sample (obtained from Arabian Ladina for Industries Co. Ltd., Jeddah, Saudi Arabia), denoted as PM0, was fabricated by dissolving 1 g of PS in 4 mL of toluene. The mixture was thoroughly mixed through rough sonication to ensure homogeneity and transferred to a silicon mold. It was left to solidify for 24 h to obtain the desired shape and form. The composite samples were prepared as follows: 1 mg of (2-methyl-9,10-bis(naphthalen-2-yl)anthracene), commonly known as MADN (obtained from Ossila Ltd, Sheffield, UK), was dissolved in toluene and sonicated for 10 min. Different proportions of the solution were dispersed on the PS matrix and sonicated for 30 min. Subsequently, the composites were transferred to molds and left to solidify in the required shape and form. These samples are denoted as PM1–PM5. ZnO with a density of 5.61 g/cm^3 was obtained from the Intermediate Chemicals Company-ARABIAN ZINC, Riyadh, Saudi Arabia. Different amounts of the ZnO nanoparticles were added and mixed with the MADN–PS matrix and sonicated for 30 min to obtain the PMZnO1–PMZnO5 samples. The mixture was sonicated for an additional 30 min to distribute the particles evenly and make the composite more homogeneous. Finally, the homogenized mixture was placed in molds to obtain square-shaped samples of varying thicknesses—2 mm, 4 mm, and 5 mm—for each sample type. The density (ρ) of the samples was determined by dividing the mass (m) of each sample (in grams) by its volume (V) (in cubic centimeters) (table 1). The error in density measurement was calculated using equation 1.

$$\Delta\rho = \rho\sqrt{\left(\frac{\Delta m}{m}\right)^2 + \left(\frac{\Delta V}{V}\right)^2} \quad (1)$$

Where; $\Delta\rho$ error in density measurement, Δm and ΔV are uncertainties in mass and volume.

Measurement of linear and mass attenuation coefficients

Three conventional point sources, ^{214}Am (59.5 keV), ^{137}Cs (661.7 keV), and ^{60}Co (1173.2 and 1332.5 keV), were used to irradiate the fabricated samples. A sodium iodide (NaI (TI)) scintillation detector (2"×2") was used to measure the energy intensity. The system was protected from background radiation and scattering by a lead shielding container. Gamma spectra were analyzed and detected using the

[DOI: 10.61186/ijrr.23.4.23]

Maestro-ORTEC. All samples were subjected to radiation for precisely 2700 s to guarantee accurate statistical findings. As shown in figure 1, two Ø 0.3 cm collimators were used in front of the source and detector, respectively. Both collimators were made of 1 cm-thick lead in the form of a disc, with a perforated center hole of Ø 0.3 cm. The point source and sample were separated by 9.2 cm, whereas the point source and detector were separated by 14.8 cm. Subsequently, the source was positioned, and the first gamma radiation, denoted as I_o, was detected. Gamma counts were established for each material at various thicknesses. To obtain an objective assessment, the relative counts (I/I_o) were computed for various thicknesses and analyzed.

Table 1. Compositions of fabricated samples with different additives.

Samples Code	Concentration (wt.%)			Measured density (g/cm^3)
	Polystyrene	MADN	ZnO	ρ ± Δρ
PM0	100.00	0.00	0.00	0.87±0.01
PM1	98.12	1.88	0.00	0.88±0.01
PM2	96.23	3.77	0.00	0.88±0.01
PM3	94.35	5.65	0.00	0.88±0.01
PM4	92.47	7.53	0.00	0.88±0.01
PM5	90.58	9.42	0.00	0.89±0.01
PMZnO1	92.47	5.65	1.88	0.96±0.02
PMZnO2	90.58	5.65	3.77	1.05±0.02
PMZnO3	88.70	5.65	5.65	1.13±0.03
PMZnO4	86.82	5.65	7.53	1.22±0.03
PMZnO5	84.93	5.65	9.42	1.30±0.03

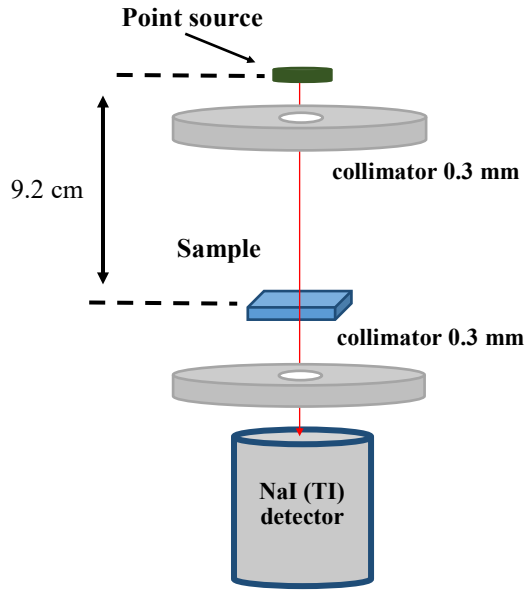

Figure 1. Schematic of the experimental setup.

Using Beer–Lambert's law, we calculated the mass attenuation coefficient $\boldsymbol{\mu/\rho}$ (cm^2/g) by dividing the linear attenuation coefficient by the sample's density, as shown in equation 2:

$$\mu/\rho = \frac{1}{\rho x}\ln\left(\frac{I_o}{I}\right) \quad (2)$$

Where; $\boldsymbol{I_o}$ is the photon intensity before attenuation, $\boldsymbol{I}$ is the photon intensity after attenuation, and $\boldsymbol{\rho x}$ is the area density of the mass.

The error of $\Delta\,\mu/\rho$ measurement is calculated using equation 3

$$\frac{\Delta\mu/\rho}{\mu/\rho} = \sqrt{\left(\frac{\Delta m_\rho}{m_\rho}\right)^2 + \left(\frac{\Delta I}{I}\right)^2 + \left(\frac{\Delta I_o}{I_o}\right)^2} \quad (3)$$

Where; Δm_ρ ,ΔI_o and ΔI are the error of the mass density, unattenuated photon intensity and attenuated photon intensity, respectively.

The half value layer (HVL) is the thickness required to cut the amount of radiation in half and is calculated as shown in equation 4:

$$HVL = \frac{ln2}{\mu} \quad (4)$$

Where; $\boldsymbol{\mu}$ is the linear attenuation coefficient (cm^{-1}).

The distance traveled by a photon before it interacts with something is called its mean free path (MFP). The MFP can be determined by taking the inverse of the linear absorption coefficient of the sample material, as shown in equation 5:

$$MFP = \frac{1}{\mu} \quad (5)$$

RESULTS

Linear and Mass attenuation coefficient measurements

The linear (μ) and mass attenuation coefficients (μ/ρ) of the fabricated PS composites were measured at photon energies of 59.5 keV, 661.7 keV, 1173.2 keV, and 1332.5 keV. The first intensity, I_o, which serves as the reference value for each sample was measured considering a specific photon energy and duration. The fabricated materials were then positioned between the source and the detector to measure the transmitted intensity (I). The linear attenuation coefficient was calculated from this value considering varying material thicknesses. Two groups of samples were evaluated: PM0–PM5, which contained varying concentrations of the conjugated hole transport material (MNPA), and PMZnO1–PMZnO5, which contained a fixed MNPA concentration (5.6%) and varying amounts of ZnO. The results are summarized in table 2. At lower photon energies, such as at 59.5 keV, all samples exhibited high μ/ρ values, which decreased as the photon energy increased. This trend was more pronounced in the samples containing ZnO, highlighting the effect of the high atomic number of zinc on photon interactions. In the medium- to high-energy range (661.7 keV to 1332.5 keV), the μ/ρ values of all the samples gradually decreased, reflecting the dominance of Compton scattering at these energies.

The PM0–PM5 samples demonstrated minimal variation in their μ/ρ values across different MNPA

[DOI: 10.61186/ijrr.23.4.23]

concentrations, indicating that the Low-Z elements (carbon and hydrogen) in MNPA provided limited attenuation. For instance, at 59.5 keV, the μ/ρ values of the samples ranged from 0.171 cm^2/g (PM4) to 0.176 cm^2/g (PM2), with an error of ±0.0033 cm^2/g, emphasizing the stability across this sample group. In contrast, the PMZnO1–PMZnO5 samples exhibited a marked increase in both μ and μ/ρ, particularly at lower photon energies. For instance, at 59.5 keV, the μ/ρ value increased from 0.176 cm^2/g in PM0 (without ZnO) to 0.283 cm^2/g in PMZnO5 (with 9.42% ZnO), reflecting the photoelectric absorption of ZnO. At 1332.5 keV, the μ/ρ values remained higher for the ZnO-enhanced samples, ranging from 0.059 cm^2/g in PM0 to 0.076 cm^2/g in PMZnO5. These results suggest that ZnO's higher atomic number and increased electron density enhance photon interactions, especially at lower energy levels. Figure 2 depicts these variations, showing the attenuation performance of the composites across different energy ranges.

Table 2. Linear and mass attenuation coefficients of the fabricated samples.

	59.5 keV			661.7 keV			1173.2 keV			1332.5 keV		
Sample	**μ**	**μ/ρ**	**±σ(μ/ρ)**	**μ**	**μ/ρ**	**±σ(μ/ρ)**	**μ**	**μ/ρ**	**±σ(μ/ρ)**	**μ**	**μ/ρ**	**±σ(μ/ρ)**
PM0	0.154	0.176	0.0033	0.070	0.080	0.0017	0.055	0.063	0.0629	0.052	0.059	0.0010
PM1	0.154	0.175	0.0026	0.070	0.080	0.0021	0.055	0.063	0.0626	0.052	0.059	0.0013
PM2	0.154	0.176	0.0029	0.069	0.079	0.0017	0.055	0.062	0.0622	0.052	0.059	0.0012
PM3	0.153	0.174	0.0029	0.071	0.080	0.0013	0.055	0.062	0.0623	0.052	0.059	0.0008
PM4	0.151	0.171	0.0028	0.070	0.079	0.0019	0.055	0.062	0.0622	0.052	0.059	0.0015
PM5	0.153	0.172	0.0035	0.070	0.078	0.0017	0.055	0.062	0.0618	0.052	0.059	0.0008
PMZnO 1	0.191	0.198	0.0041	0.077	0.080	0.0017	0.060	0.062	0.0625	0.057	0.059	0.0014
PMZnO 2	0.230	0.220	0.0068	0.084	0.080	0.0014	0.065	0.062	0.0621	0.062	0.059	0.0013
PMZnO 3	0.269	0.237	0.0063	0.090	0.079	0.0017	0.070	0.062	0.0616	0.066	0.058	0.0016
PMZnO 4	0.320	0.263	0.0047	0.097	0.080	0.0019	0.075	0.061	0.0614	0.071	0.059	0.0020
PMZnO 5	0.368	0.283	0.0077	0.104	0.080	0.0027	0.080	0.062	0.0618	0.076	0.058	0.0010

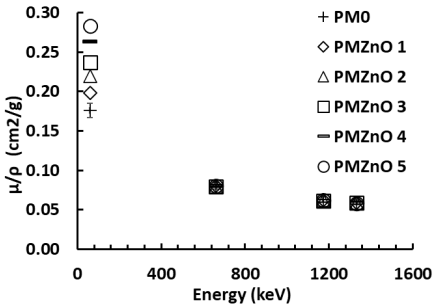

Figure 2. Mass attenuation coefficient (μ/ρ) as a function of photon energy for polystyrene (PS) integrated with ZnO.

Figure 3 compares the linear attenuation coefficients of PS samples with different amounts of conjugated hole transport material with those of PS samples with a PM ratio of 50% and different amounts of ZnO at photon energies of 59.5 keV, 661.7 keV, 1173.2 keV, and 1332.5 keV. For PM material concentrations of 1.88%–9.42%, the linear attenuation coefficients at all the measured photon energies are relatively close. This is because the added conjugated hole transport material does not significantly alter the linear attenuation coefficient of the PS. The linear attenuation coefficient at the measured energies is higher with the addition of ZnO, and increasing the percentage of the ZnO additive enhances its effect on the linear attenuation coefficient. If small amounts of ZnO are added, it may not have a significant effect on the overall attenuation properties of the compound. This may be attributed to the lack of uniform distribution of ZnO within the PS matrix when it is added at lower concentrations (1.88% and 3.77%).

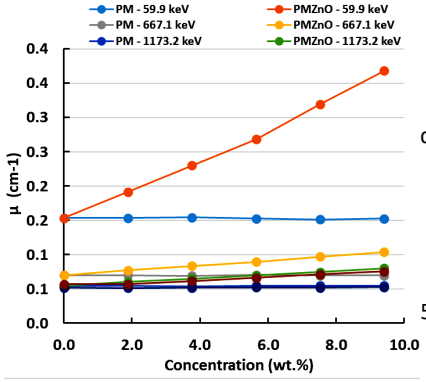

Figure 3. Linear attenuation coefficient μ of PS composites with different conjugated hole transport material (PM) and ZnO (PMZnO) concentrations, at photon energies of 59.5 keV, 661.7 keV, 1173.2 keV, and 1332.5 keV.

Table 3. Comparison of half value layer (HVL) of mate-rials from this and other studies at 661.7 keV.

Materials	Study theme	HVL (cm)
PMZnO 5 (current work)	Experimental	6.667
HDPE - (10%) ZnO [29]	Experimental	7.220
Polystyrene (PS) [30]	Calculated	8.027
Polyethylene (PE) [30]	Calculated	8.363
Polypropylene (PP) [30]	Calculated	8.318
Polyacrylamide - 5% ZnO [31]	Simulation	6.330

Half value layer (HVL)

The HVL, which is the material thickness required to reduce photon intensity by half, further demonstrates the influence of ZnO on the composite's shielding properties. For the PM0–PM5 samples, the HVL values were relatively stable across all energy levels, reflecting the minimal impact of MNPA on photon attenuation. At 59.5 keV, HVL ranged from 4.486 cm for PM2 to 4.578 cm for PM4. The addition of ZnO significantly reduced the HVL values of the

[DOI: 10.61186/ijrr.23.4.23]

PMZnO samples, particularly at lower energies. For instance, at 59.5 keV, the HVL decreased from 4.509 cm in PM0 to 1.882 cm in PMZnO5, indicating enhanced photon absorption at higher ZnO contents. This reduction in HVL was consistently observed across the energy spectrum, although it was less pronounced at higher energies; at 1332.5 keV, the HVL decreased from 13.378 cm for PM0 to 9.157 cm for PMZnO5. The HVL curves of the composites with varying concentrations of ZnO and MADN are shown in figure 4.

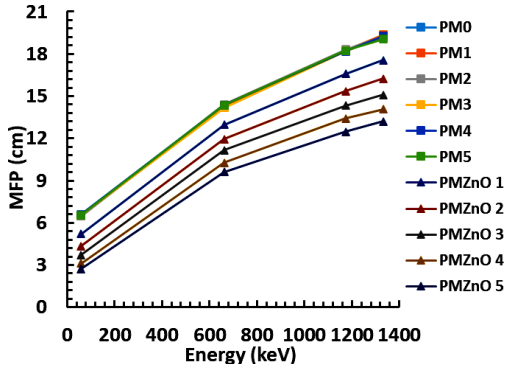

Figure 5. The mean free path (MFP) of the polystyrene (PS) samples integrated with the conjugate hole transport material and ZnO at photon energies of 59.5 keV, 661.7 keV, 1173.2 keV, and 1332.5 keV.

Table 3 shows that PMZnO5 has a higher attenuation effectiveness with an HVL of 6.667 cm compared to pure polymers like polystyrene (HVL = 8.027 cm), polyethylene (HVL = 8.363 cm), and polypropylene (HVL = 8.318 cm) at 661.7 keV. This highlights the poor shielding capacity of Low-Z materials, and the notable improvement in shielding capacity due to ZnO addition, which boosts photon interactions through Compton scattering and photoelectric absorption. PMZnO5 also outperforms HDPE-ZnO (10%), which has an HVL of 7.220 cm, thereby highlighting the efficiency of integrating ZnO in a polystyrene matrix. The experimental HVL value of PMZnO5 is close to the simulated HVL value of polyacrylamide-ZnO (5%) (6.330 cm), highlighting its dependable performance in practical settings. Thus, ZnO-enhanced PS composites can serve as effective, lightweight materials for radiation shielding.

Mean free path (MFP)

The MFP, which represents the average distance traveled by photons before interacting with the material, was measured for all the samples. For the PM0–PM5 samples, the MFP values exhibited only minor variation, similar to that of the HVL values. At 59.5 keV, the MFP ranged from 6.473 cm in PM2 to 6.606 cm in PM4. The limited variation reflects the low atomic numbers of MNPA and PS, which contribute minimally to photon attenuation. In contrast, the samples with ZnO exhibited substantially lower MFP values, particularly at low photon energies, as shown in Figure 5. At 59.5 keV, the MFP decreased from 6.507 cm in PM0 to 2.716 cm in PMZnO5. This indicates increased attenuation efficiency owing to the high atomic number of Zn. This trend persisted across energy levels, although it diminished at higher energies. At 1332.5 keV, the MFP decreased from 19.304 cm for PM0 to 13.213 cm for PMZnO5. Thus, ZnO enhances photon interaction density within the composite, effectively reducing the photon penetration distance.

DISCUSSION

This study highlights the significant impact of material composition on the radiation attenuation properties of polystyrene (PS) composites, with a specific focus on the synergistic effects of MNPA and ZnO. The findings show that MNPA–PS composites (PM0 - PM5) exhibited limited improvements in attenuation properties, with the mass attenuation coefficient (μ/ρ) at 59.5 keV consistently around 0.176 cm^2/g. The low atomic numbers of carbon and hydrogen cause this behavior. These atomic numbers control how photons interact with these materials, which is supported by previous research on low-Z polymer composites [29]. Although MNPA improves the structural and physical properties of PS, it does not significantly enhance radiation attenuation, as its low atomic number limits its interaction with photons, particularly at lower energies where the photoelectric effect dominates.

Incorporating ZnO into the PS composites (PMZnO1–PMZnO5) significantly enhanced their attenuation performance. At 59.5 keV, the mass attenuation coefficient increased from 0.176 cm^2/g for PM0 to 0.283 cm^2/g for PMZnO5, a 60.8% improvement. This enhancement results from the high atomic number of zinc (Z = 30), which increases photoelectric absorption, as similarly observed in studies on HDPE/ZnO composites [12]. Additionally, the half-value layer (HVL) and mean free path (MFP) decreased significantly with ZnO addition. At 59.5 keV, the HVL for PMZnO5 was reduced to 1.882 cm compared to 4.509 cm for PM0, and the MFP decreased from 6.507 cm to 2.716 cm. These smaller amounts show better photon absorption and scattering, which is in line with earlier research that showed how high-Z additives can improve radiation shielding [30-32].

ZnO-enhanced composites have several benefits over conventional lead-based shielding materials, such as reduced weight, environmental safety, and adaptability. Although lead serves as an efficient barrier, its toxicity and density limit its use in contexts necessitating portable or lightweight materials. ZnO-enhanced PS composites provide a safer and more sustainable alternative, appropriate for applications like medical imaging equipment, portable radiation shields, and nuclear facility barriers. These composites exhibit remarkable

[DOI: 10.61186/ijrr.23.4.23]

flexibility and structural integrity, making them suitable for contemporary radiation shielding requirements [33].

The homogenous distribution of ZnO nanoparticles inside the PS matrix is essential for attaining uniform and improved attenuation characteristics. Future investigations should concentrate on integrating ZnO with other high-Z additions, such as tungsten or bismuth, to enhance shielding efficacy while also assessing the long-term durability and resilience of these composites under diverse environmental conditions and radiation exposures. ZnO-enhanced PS composites combine the structural benefits of MNPA with the high-Z properties of ZnO. This makes radiation shielding materials that are light, effective, and flexible. These discoveries provide a basis for safer and more versatile alternatives to conventional materials, facilitating future advancements in radiation shielding technology.

CONCLUSION

This study highlights the critical role of material composition in radiation attenuation. While MNPA–PS composites (PM0–PM5) showed consistent attenuation coefficients due to their low atomic number components, the addition of ZnO significantly improved performance. At 59.5 keV, ZnO -enhanced composites (PMZnO5) exhibited a mass attenuation coefficient (μ/ρ) of 0.283 cm^2/g, reducing the half-value layer (HVL) from 4.509 cm to 1.882 cm and the mean free path (MFP) from 6.507 cm to 2.716 cm. These results demonstrate the potential of ZnO-enhanced PS composites as lightweight and effective radiation shielding materials for medical, industrial, and nuclear applications.

Funding: This work was conducted without any financial support.

Conflicts of Interests: The authors declare no conflicts of interest.

Ethical Considerations: This study did not involve human participants or animals and did not require ethical approval.

Author Contribution: M.M.: Conceptualization, methodology, data collection, formal analysis, investigation, writing-original draft preparation. M.A.: Validation, methodology, writing-review & editing, resources.

AI Usage: No Artificial Intelligence tools were used in the creation or preparation of this manuscript.

REFERENCES

1. Zou Y, Wei Y, Wang G, Meng F, Gao M, Storm G, Zhong Z (2017) Nanopolymersomes with an ultrahigh iodine content for high-performance X-ray computed tomography imaging in vivo. *Adv Mater*, ***29****(10): 1603997*.
2. Howard JA and Probert MR (2014) Cutting-edge techniques used for the structural investigation of single crystals. *Science*, ***343*** *(6175): 1098-1102*.
3. Durante M and Cucinotta FA (2011). Physical basis of radiation protection in space travel. *Reviews of Modern Physics*, ***83****(4): 1245*.
4. Bakar NFA, Othman SA, Azman NFAN, Jasrin NS (2019) Effect of ionizing radiation towards human health: A review. In IOP Conference Series: *Earth and Environmental Science,* ***268****(1): 012005*. IOP Publishing.
5. Almurayshid M, Helo Y, Kacperek A, Griffiths J, Hebden J, Gibson A (2017) Quality assurance in proton beam therapy using a plastic scintillator and a commercially available digital camera. Journal of Applied Clinical Medical Physics, **18**(5): 210-219.
6. AbuAlRoos NJ, Azman MN, Amin NAB, Zainon R (2020) Tungsten-based material as promising new lead-free gamma radiation shielding material in nuclear medicine. *Physica Medica*, ***78****: 48-57*.
7. Khosravi H, Sani KG, Jafari S, Nikzad S (2023) Evaluation of the radiation protection capability of a low density and non-Lead composite shield using Monte Carlo model. *International Journal of Radiation Research*, ***21****(4): 833-836*.
8. Abdolahzadeh T, Morshedian J, Ahmadi S (2023) Novel polyethylene/tungsten oxide/bismuth trioxide/barium sulfate/ graphene oxide nanocomposites for shielding against X-ray radiations. *International Journal of Radiation Research*, ***21****(1): 79-87*.
9. Al Hassan M, Liu WB, Wang J, Ali MMM, Rawashdeh A (2022) Monte Carlo simulations of gamma-rays shielding with phthalonitrile-tungsten borides composites. *International Journal of Radiation Research*, ***20****(3): 621-626*.
10. Lee JB, Byun JI, Yun JY (2020) Mass attenuation coefficients of environmental samples for gamma-ray energies from 46.5 keV to 1408 keV. *International Journal of Radiation Research*, ***18****: 201-207*.
11. Vagheian M, Sardari D, Saramad S, Ochbelagh DR (2020). Experimental and theoretical investigation into X-ray shielding properties of thin lead films. *International Journal of Radiation Research*, ***18****(2): 263-274*.
12. Alshareef R, Marashdeh MW, Almurayshid M, Alsuhybani M (2023) Study of radiation attenuation properties of HDPE/ZnO at energies between 47.5 and 266 keV. *Progress in Nuclear Energy*, ***165****: 104909*.
13. Hussein M, Dannoun A, Aziz EM, Brza SB, Abdulwahid MA, Hussen RT, *et al.* (2020) Steps toward the band gap identification in polystyrene based solid polymer nanocomposites integrated with tin titanate nanoparticles. *Polymers*, ***12****(10): 2320*.
14. Cinan ZM, Erol B, Baskan T, Mutlu S, Ortaç B, Savaskan Yilmaz S, Yilmaz AH (2022) Radiation shielding tests of crosslinked polystyrene-b-polyethyleneglycol block copolymers blended with nanostructured selenium dioxide and boron nitride particles. *Nanomaterials*, ***12****(3): 297*.
15. Brandrup J, Immergut EH, Grulke EA, Abe A, Bloch DR (Eds.) (1999). Polymer handbook (Vol. 89). New York: Wiley.
16. Al-Buriahi MS, Eke C, Alomairy S, Yildirim A, Alsaeedy HI, Sriwunkum C (2021) Radiation attenuation properties of some commercial polymers for advanced shielding applications at low energies. *Polymers for Advanced Technologies*, ***32****(6): 2386-2396*.
17. Körpinar B, Canbaz B, Füsun ÇAM, Hakan AKAT (2021) Gamma radiation shielding and thermal properties of the polystyrene/ tungsten (VI) oxide composites. *Erzincan University Journal of Science and Technology*, ***14****(2): 395-407*.
18. Cinan ZM, Erol B, Baskan T, Mutlu S, Savaskan Yilmaz, S, Yilmaz AH (2021) Gamma irradiation and the radiation shielding characteristics: For the lead oxide doped the crosslinked polystyrene-b-polyethyleneglycol block copolymers and the polystyrene-b-polyethyleneglycol-boron nitride nanocom-posites. *Polymers*, ***13****(19): 3246*.
19. Osman AF, El Balaa H, El Samad O, Awad R, Badawi MS (2023) Assessment of X-ray shielding properties of polystyrene incorporated with different nano-sizes of PbO. *Radiation and Environmental Biophysics*, ***62****(2): 235-251*.
20. Azmi R, Nam SY, Sinaga S, Akbar ZA, Lee CL, Yoon SC, *et al.* (2018) High-performance dopant-free conjugated small molecule-based hole-transport materials for perovskite solar cells. *Nano Energy*, ***44****: 191-198*.
21. Xie Z, Park H, Choi S, Park HY, Gokulnath T, Kim H, *et al.* (2023) Thienothiophene-assisted property optimization for dopant-free π-conjugation polymeric hole transport material achieving over 23% efficiency in perovskite solar cells. *Advanced Energy Materials*, ***13*** *(2): 2202680*.

[DOI: 10.61186/ijrr.23.4.23]

22. Zhang F, Liu X, Yi C, Bi D, Luo J, Wang S, *et al.* (2016) Dopant-free donor (D)–π–D–π–D conjugated hole-transport materials for efficient and stable perovskite solar cells. *ChemSusChem*, ***9****(18): 2578-2585*.
23. Wang J, Wang S, Li X, Zhu L, Meng Q, Xiao Y, Li D (2014) Novel hole transporting materials with a linear π-conjugated structure for highly efficient perovskite solar cells. *Chemical Communications*, ***50****(44): 5829-5832*.
24. Shih CC, Chiang YC, Hsieh HC, Lin YC, Chen WC (2019) Multilevel photonic transistor memory devices using conjugated/insulated polymer blend electrets. *ACS Applied Materials & Interfaces*, ***11*** *(45): 42429-42437*.
25. Oyama K, Seike M, Mitamura K, Watase S, Suzuki T, Omura T, *et al.* (2021) Monodispersed nitrogen-containing carbon capsules fabricated from conjugated polymer-coated particles via light irradiation. *Langmuir*, ***37****(15): 4599-4610*.
26. Brabec CJ, Padinger F, Sariciftci NS, Hummelen JC (1999) Photovoltaic properties of conjugated polymer/methanofullerene composites embedded in a polystyrene matrix. *Journal of Applied Physics*, ***85****(9): 6866-6872*.
27. Beek WJ, Wienk MM, Janssen RA (2004) Efficient hybrid solar cells from zinc oxide nanoparticles and a conjugated polymer. *Advanced Materials*, ***16****(12): 1009-1013*.
28. Beek WJ, Wienk MM, Kemerink M, Yang X, Janssen RA (2005) Hybrid zinc oxide conjugated polymer bulk heterojunction solar cells. *The Journal of Physical Chemistry B*, ***109****(19): 9505-9516*.
29. Nambiar S and Yeow JT (2012) Polymer-composite materials for radiation protection. *ACS Applied Materials & Interfaces*, ***4****(11): 5717-5726*.
30. Alsayed Z, Badawi MS, Awad R, Thabet AA, El-Khatib AM (2019) Study of some γ-ray attenuation parameters for new shielding materials composed of nano ZnO blended with high density polyethylene. *Nuclear Technology and Radiation Protection*, ***34****(4): 342-352*.
31. Mirji, R and Lobo B (2017) Computation of the mass attenuation coefficient of polymeric materials at specific gamma photon energies. Radiation Physics and Chemistry, **135**: 32-44.
32. Nasehi F and Ismail M (2019) Evaluation of X and gamma-rays attenuation parameters for polyacrylamide and ZnO composites as light shielding materials using MCNP and X-COM simulation. *Nucl Med Radiat Ther*, ***10****(404): 2*.
33. Ponnamma D, Cabibihan JJ, Rajan M, Pethaiah SS, Deshmukh K, Gogoi JP, *et al.* (2019) Synthesis, optimization and applications of ZnO/polymer nanocomposites. *Materials Science and Engineering: C*, ***98****: 1210-1240*.

[DOI: 10.61186/ijrr.23.4.23]